International Journal of Mass Spectrometry 279 (2009) 113–118

Contents lists available at ScienceDirect

International Journal of Mass Spectrometry

journal homepage: www.elsevier.com/locate/ijms

Collision-induced dissociation of tetraphenyl iron and manganese porphyrin ions by electrospray ionization mass spectrometry

Tuba Gozet, Lise Huynh, Diethard K. Bohme*

Department of Chemistry, Centre for Research in Mass Spectrometry and Centre for Research in Earth and Space Science, York University, 4700 Keele St., Toronto, Ontario, Canada M3J 1P3

ARTICLE INFO

Article history:
Received 30 August 2008
Received in revised form 24 October 2008
Accepted 25 October 2008
Available online 5 November 2008

Keywords:
Electrospray ionization
Collision-induced dissociation
Metalloporphyrins
Hydrogen loss

ABSTRACT

Tetraphenyl iron(III) and manganese(III) porphyrin chloride (FeTPPCl and MnTPPCl) are studied by electrospray ionization tandem mass spectrometry (ESI/MS/MS). Removal of the chloride counter ion from these salts results in intense $[FeTPP]^+$ and $[MnTPP]^+$ ions that lose hydrogen and peripheral phenyl rings upon multi-collision-induced dissociation (CID). Dissociation pathways are probed as a function of collision-offset voltage with onset measurements. Onset voltages generally are higher for $[MnTPP]^+$. While primary losses of benzene, biphenyl and hydrogen occur concomitantly at low collision voltages, losses of hydrogen from the secondary and higher-order ions occur at higher collision voltages. Comparisons are made with previous measurements using surface-induced dissociation, photodissociation and electron impact.

1. Introduction

The biological importance of metalloporphyrins, especially manganese and iron derivatives of porphyrins, is well known [1,2]. Iron porphyrins constitute the prosthetic groups in heme proteins and are involved in the transport and storage of oxygen in the hemoglobins and myoglobins [3–8], in electron transfer in the cytochromes [9], and in the catalysis of peroxide decomposition and activation. Manganese porphyrins are used for the oxidation of olefins [10,11], for oxidative cleavage of DNA [10,12,13] and for removal of superoxide anions in mammalian cells [14].

The porphyrin macrocycle is composed of a tetrapyrrolic unit and has square planar geometry because of electronic delocalization. The dianionic porphinato ligand forms by removal of two central protons and acts as a tetradentate ligand for metal cations. So the minimum coordination number in metalloporphyrins is four. Neutral, anionic or cationic ligation of the metal in the axial position usually results in 5 or 6 coordinated metalloporphyrins that have a square pyramidal geometry. In FeTPPCl and MnTPPCl a negatively charged axial Cl^- ligand balances the positive charge on the metal in a square pyramidal five coordinate structure (see Scheme 1). The Mn(III) in MnTPPCl and the Fe(III) in FeTPPCl have a high spin with electronic configurations of d^4 and d^5, respectively. X-ray crystallography shows that both FeTPPCl and MnTPPCl are non-planar with the metal pushed out of plane and the chloride counter ion in the axial position [15,16].

The ionization and dissociation of metalloporphyrins of the type MTPP(Cl) (M = metal) have been characterized with various ionization and mass spectrometric techniques. Gas phase $[Fe/MnTPP]^+$ ions were first produced in 1989 by laser desorption and ionization (LDI) of Fe/MnTPPCl. Fragmentation of these molecular ions was achieved both by photodissociation (PD) at 308 nm (4.03 eV) [17], 388 nm (3.20 eV) and 575 nm (2.16 eV) [18] and by surface-induced dissociation (SID) at 69 eV, 139 eV, and 278 eV [19], as well as 36 eV, 72 eV and 144 eV [18]. Only recently have $[FeTPP]^+$ and its fragmentation products been obtained by electron impact (EI) ionization [20]; FeTPPCl powder was vaporized in an oven at 300 °C and the neutral vapor molecules exposed to an electron beam (at 70 eV). Qualitatively the three different techniques of ion dissociation (LDI, SID, EI) show similar fragmentation behavior: dissociation of $[MTPP]^+$ occurs primarily by loss of benzene, two benzenes, two phenyl groups and hydrogen molecules. Minor amounts of C_6H_5 (EI), $(C_6H_6 + C_6H_5)$ (PD, EI) and successive losses of hydrocarbons (PD, SID, EI), also have been reported.

Here we report studies of the direct dissociation of $[MTPP]^+$ ions using electrospray ionization and collision-induced dissociation (ESI/MS/MS). The $[MTPP]^+$ ions are born in solution as the parent salt dissociates by heterolytic cleavage (induced by solvent molecules) [21], are sprayed into the gas phase and are then dissociated by collisions with N_2 molecules as a function of collision energy. In the previous studies of $[Fe/MnTPP]^+$ by PD and SID, dissociation is limited to only a few energies [17–19]. In SID the ions

* Corresponding author. Tel.: +1 416 736 2100; fax: +1 416 736 5936.
E-mail address: dkbohme@yorku.ca (D.K. Bohme).

1387-3806/$ – see front matter © 2008 Elsevier B.V. All rights reserved.
doi:10.1016/j.ijms.2008.10.018

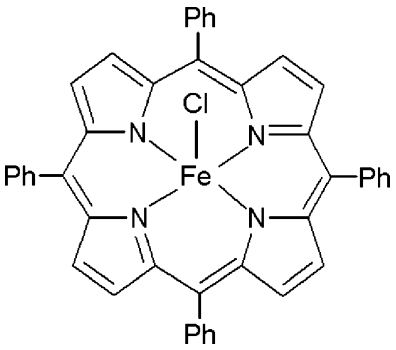

Scheme 1. .

collide with a solid surface (stainless steel) instead of gas molecules at discrete collision energies (69 eV, 139 eV, 278 eV [19], 36 eV, 72 eV and 144 eV [18]). In PD, the parent molecules are fragmented by photon absorption and, similar to SID, fragmentation has been performed only at certain radiation energies (308 nm [17], 388 nm [18] and 575 nm [18]). Electron energies of 70 eV are employed in EI and molecular and fragment ions are produced concomitantly. In comparison, with the ESI/MS/MS technique the direct dissociation of the $[MTPP]^+$ ions is monitored using MS/MS in small steps of energy over a large range of collision energies and breakdown occurs sequentially with increasing energy.

The direct dissociation of MTPP appears not to have been studied previously by ESI/MS/MS, although $[MTPP]^+$ ions have been observed in the ESI/MS spectra of tetraphenylporphyrins [22] and mentioned as product ions in the collision-induced dissociation of some $[Fe/MnTPP]^+$/ligand complexes [23,24]. Also, metalloporphyrins of octaethylporphyrin have been analyzed by ESI/MS

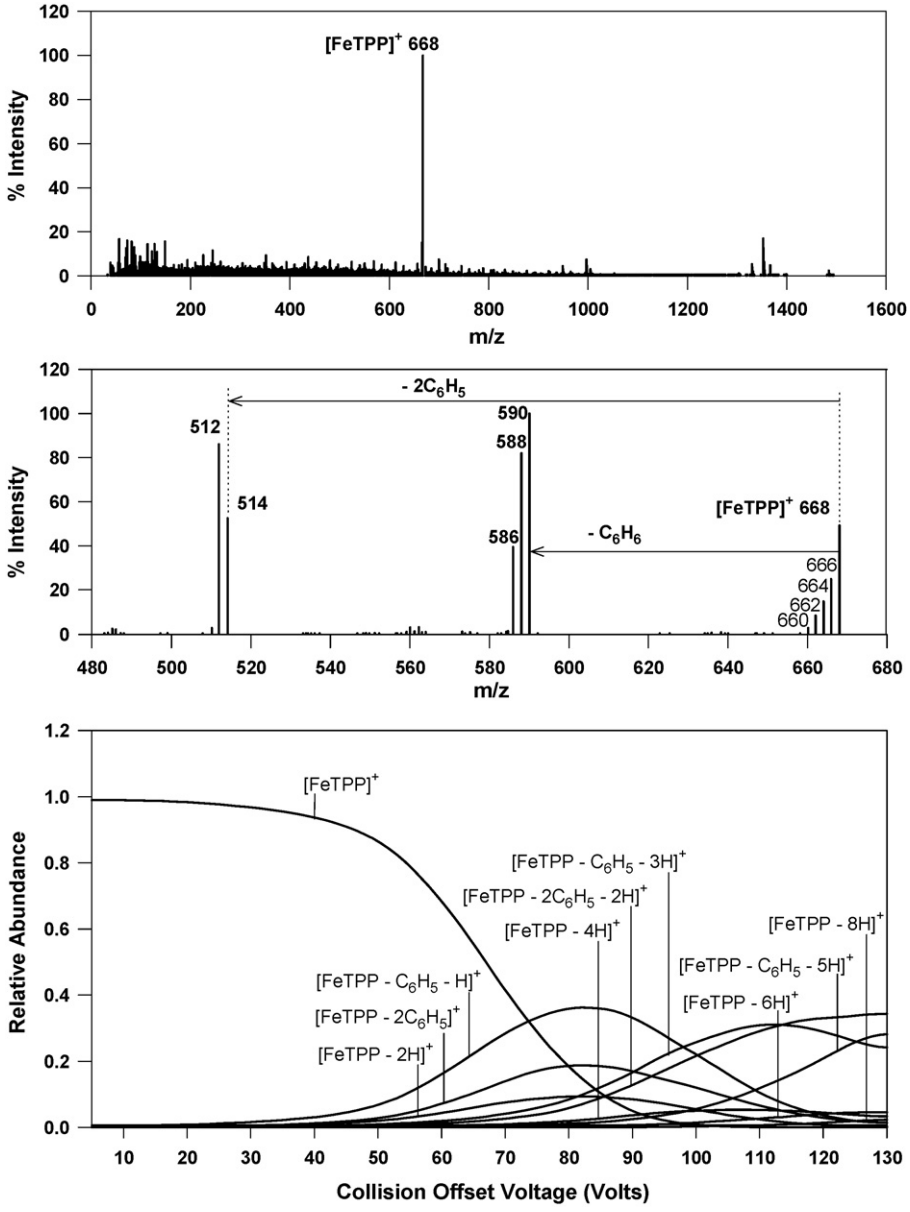

Fig. 1. ESI/MS spectrum of FeTPPCl (top), CID spectrum of $[FeTPP]^+$ (middle) averaged over the range from 65 V to 130 V, and CID profiles monitored for the dissociation of $[FeTPP]^+$ (bottom). The raw MRM curves are shown as Supplementary Data.

[22,25] and EI/MS [26]. Dissociation of the ions was investigated by CID [25,26] and showed the losses of ethyl and methyl groups.

2. Experimental

Experiments were preformed with a triple quadruple mass spectrometer [27] equipped with an ESI interface, an API 2000 (MDS SCIEX, Concord, Ontario) [28,29]. 1–10 μM solutions of FeTPPCl/CH_3OH and MnTPPCl/CH_3CN were prepared by dissolving FeTPPCl and MnTPPCl in CH_3OH and CH_3CN, respectively. MnTPPCl was found to be soluble in both CH_3CN and CH_3OH but FeTPPCl only in CH_3OH. The ESI/MS results obtained with the MnTPPCl/CH_3OH solution are consistent with those obtained with the MnTPPCl/CH_3CN solution with respect to the formation and dissociation of the parent ion and did not provide additional information. The sample solutions were infused continuously into the electrospray probe at a flow rate of 3–10 μL min^{-1} by means of a syringe pump. The ESI needle voltage was set to 5500 V for all experiments. The declustering potential (DP) was adjusted between 10 V and 150 V for the direct mass spectra of the samples. ESI/MS spectra were collected in the positive ion detection mode with unit and high resolution. Collision-induced dissociation (CID) experiments were carried out in the product ion (MS/MS) and multiple reaction monitoring (MRM) modes. N_2 was used as a collision gas at a pressure estimated to be about 3 mTorr (viz. multi-collision conditions). The collision offset voltage (the potential difference between the quadruple entrance lens (q_0) and the collision cell quadruple (q_2)), was applied between 5 V and 130 V for the acquisition of CID spectra.

The instrument records total ion intensities only. These contain such instrumental artifacts as instabilities of the ESI ion source, electronic noise and loss of ion transmission at higher collision energies. Since these artifacts tend to obfuscate useful information, observed variations of ion intensities with collision energy (the MRM curves) were smoothed and normalized. The onset energies were determined by fitting the steepest slope of the MRM curves of intensity versus collision offset voltage in MS Excel.

3. Results

3.1. Dissociation of [FeTPP]$^+$

A very intense singly charged ion [FeTPP]$^+$ (m/z 668) was observed in the ESI/MS of FeTPPCl (see Fig. 1). The primary product ions produced by collision-induced dissociation arise from losses of (C_6H_5 + H), $2C_6H_5$ and 2H from [FeTPP]$^+$. Sequential losses of 2H from these primary products were observed as secondary and higher order channels at elevated collision voltages. Losses of ($2C_6H_5$ + 2H) with m/z 512 dominate the loss of $2C_6H_5$ at higher collision voltages. Furthermore, sequential losses of up to 8H from [FeTPP]$^+$ and 4H from [FeTPP–C_6H_5–H]$^+$ are abundant enough to be specified as significant dissociation channels. These probably correspond to losses of stable neutral molecules such as C_6H_6, $C_{12}H_{10}$ (biphenyl) and H_2.

The CID profiles indicate that [FeTPP]$^+$ begins to dissociate sharply only above 40 V. The intensities of primary product ions formed by losses of C_6H_6, $C_{12}H_{10}$ and H_2 increase in a parallel fashion with relative intensities in the order of [FeTPP–C_6H_5–H]$^+$ > [FeTPP–$2C_6H_5$]$^+$ > [FeTPP–2H]$^+$ over the entire range from 5 V to 130 V with maxima at 82 V, 82 V and 85 V, respectively. The intensities decrease by loss of H_2 to give [FeTPP–C_6H_5–3H]$^+$, [FeTPP–$2C_6H_5$–2H]$^+$ and [FeTPP–4H]$^+$, respectively. While the ions [FeTPP–C_6H_5–3H]$^+$ and [FeTPP–$2C_6H_5$–2H]$^+$ are comparable in intensity, the intensity of [FeTPP–4H]$^+$ is much lower. [FeTPP–C_6H_6–3H]$^+$ reaches a maximum at 117 V above which it fragments by losses of H_2. The maximum for [FeTPP–4H]$^+$ is detected at 110 V. Other products formed by further losses of H_2, namely [FeTPP–C_6H_5–5H]$^+$ and [FeTPP–6H]$^+$, are dominant only at very high collision voltages in the range ~90–130 V. [FeTPP–8H]$^+$ is observed with a relatively low intensity at ~110–130 V.

3.2. Fragmentation pathways and dissociation onsets for [FeTPP]$^+$

The observed fragmentation pathways for the dissociation of [FeTPP]$^+$ are depicted in Fig. 2, along with the onset voltages determined from the steepest slope of the CID curves. Losses of C_6H_6 and $C_{12}H_{10}$ are both primary channels. Loss of $C_{12}H_{10}$ seems unusual at first glance, however if $2C_6H_5$ is regarded as biphenyl, which is as stable as benzene, this channel becomes reasonable, as does the simultaneous loss of C_6H_6 and $C_{12}H_{10}$. The onset seen for [FeTPP–$2C_6H_5$–2H]$^+$ should be due to the loss of stable H_2 from the first primary product ion [FeTPP–$2C_6H_5$]$^+$. We cannot rule out the "diagonal" dissociations in Fig. 2 of [FeTPP–2H]$^+$ by loss of C_6H_6 or $C_{12}H_{10}$ and of [FeTPP–4H]$^+$ by loss of C_6H_6.

3.3. Dissociation of [MnTPP]$^+$

The ESI/MS of MnTPPCl gave rise to an intense peak at m/z 667, [MnTPP]$^+$, as was the case for [FeTPP]$^+$ (Fig. 3). The CID of

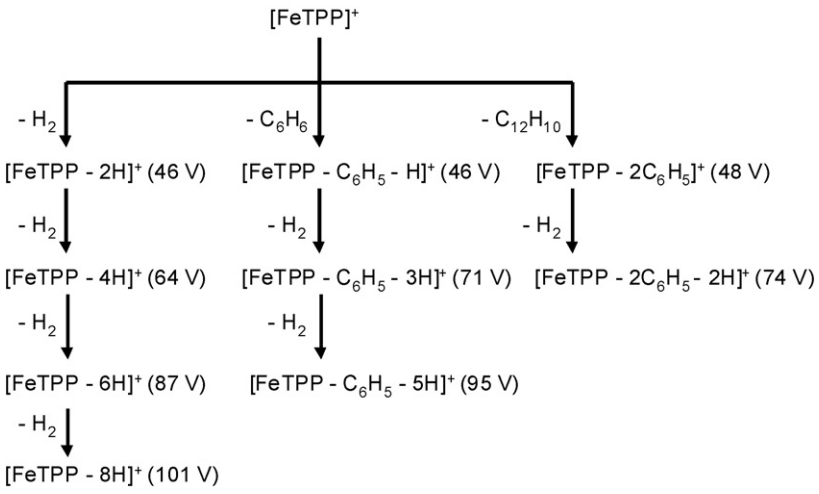

Fig. 2. Proposed dissociation channels observed for [FeTPP]$^+$. The measured onset voltages for the formation of primary and higher-order product ions are given in parentheses.

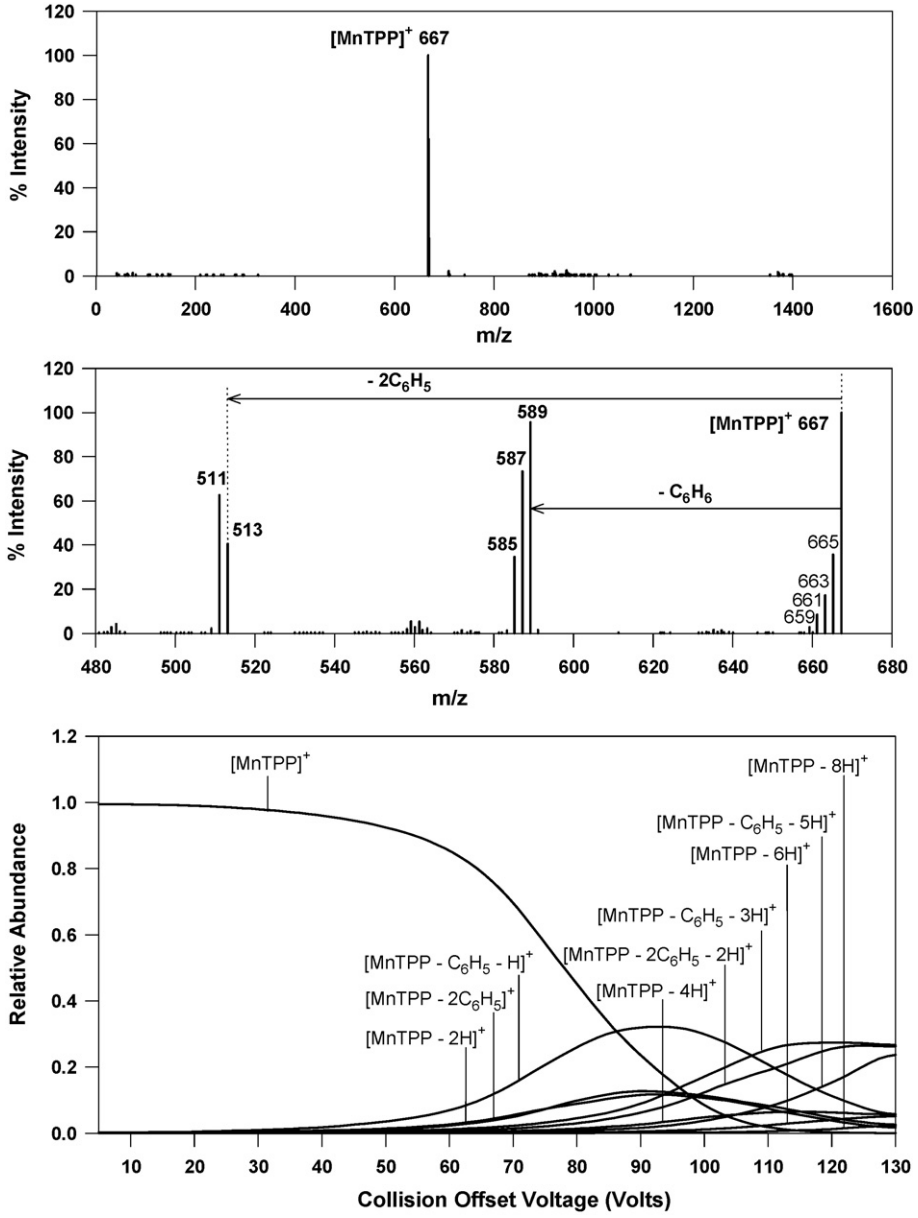

Fig. 3. ESI/MS spectrum of MnTPPCl (top), CID spectrum of $[MnTPP]^+$ (middle) averaged over the range from 65 V to 130 V, and CID profiles monitored for the dissociation of $[MnTPP]^+$ (bottom). The raw MRM curves are shown as Supplementary Data.

$[MnTPP]^+$ also exhibited similar trends as those observed with $[FeTPP]^+$ but collision voltages were shifted ~10 V higher. Losses of benzene, biphenyl and hydrogen are primary dissociation channels. Sequential losses of H_2 again occur at elevated collision voltages. The dissociation of $[MnTPP]^+$ gives rise to the appearance of $[MnTPP–C_6H_5–H]^+$, $[MnTPP–2C_6H_5]^+$ and $[MnTPP–2H]^+$. These products have maxima at 93 V, 91 V and 92 V, respectively, that can be regarded as identical. The product intensities of $[MnTPP–2C_6H_5]^+$ and $[MnTPP–2H]^+$ are essentially equal, but that of $[MnTPP–C_6H_5–H]^+$ is much higher. This dissociation behavior is different from that observed for $[FeTPP]^+$. Other channels follow the trends in dissociation observed for $[FeTPP]^+$.

3.4. Fragmentation pathways and dissociation onsets for $[MnTPP]^+$

The observed fragmentation pathways for the dissociation of $[MnTPP]^+$ are depicted in Fig. 4, along with the onset voltages. The fragmentation pathways for $[MnTPP]^+$ are similar to those observed with $[FeTPP]^+$, but the onset voltages generally are higher for $[MnTPP]^+$.

4. Discussion

4.1. Comparison of the ESI/MS/MS of $[FeTPP]^+$ and $[MnTPP]^+$

The results of our measurements indicate very similar fragmentation pathways for $[FeTPP]^+$ and $[MnTPP]^+$, but the onsets of fragmentation show an interesting difference and are higher for $[MnTPP]^+$ by ca. 10 V. Apparently Mn(III) has a greater stabilizing influence than Fe(III). Crystal structure models [15,16] and DFT calculations [30] of MnTPPCl and FeTPPCl indicate that Mn(III) is more compatible with a planar structure and fits into the porphyrin center with shorter metal–ligand bond distances while Fe(III) is further removed out of the plane of the porphyrin. Fe(III) (d^5) provides a

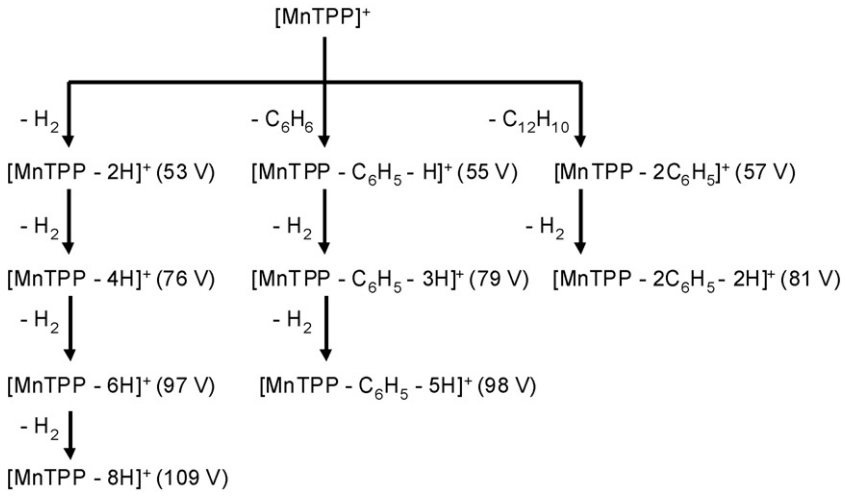

Fig. 4. Proposed dissociation channels observed for $[MnTPP]^+$. The measured onset voltages for the formation of primary and higher-order product ions are given in parentheses.

half-filled d-shell which is expected to lead to more electron repulsion by the d orbitals than with Mn(III) (d^4). This implies that there is a stronger interaction between Mn(III) and the dianionic porphinato ligand and so a greater stability against dissociation can be expected for $[MnTPP]^+$.

4.2. Comparison with SID, PD and EI

Table 1 provides a comparison of our results obtained with ESI/MS/MS with those observed with PD/FTMS [17] and EI/MS [20]. CID is different from EI and PD in the way that energy is delivered and the dissociations occur in different time frames. Energy is delivered to the molecule by fast electrons in EI and energetic photons in PD and then the molecule dissociates unimolecularly. The ionization and dissociation of the molecule occurs in a short time. In CID some of the relative kinetic energy of the ion and a colliding molecule is transferred into the internal energy and then ions with enough internal energy dissociate, or even isomerize before they dissociate. Furthermore, if multiple collisions prevail under CID operating conditions, as is often the case and also is the case here, the fragment ions may dissociate further by further collisions.

Table 1
Ions observed by LDI/PD [17], the % *I* of the ions obtained by EI [20], and the % *I* of the ions obtained by ESI/CID.[a] Ions are grouped according to the extent of loss of benzene residues. The EI results [20] are corrected for isotopic contributions. Isotopic contributions are not taken into account in the ESI/CID results (due to inadequate resolution).

Ions	LDI/PD (308 nm)	EI (70 eV)	ESI/CID (65–130 V)	
	[FeTPP]Cl and [MnTPP]Cl	[FeTPP]Cl	$[FeTPP]^+$	$[MnTPP]^+$
$[Fe/MnTPP]^+$	•	92.4	45.5	61.5
$[Fe/MnTPP–2H]^+$	•	3.2	25.7	21.9
$[Fe/MnTPP–4H]^+$	•	1.8	16.8	10.2
$[Fe/MnTPP–6H]^+$	•	–	9.0	4.7
$[Fe/MnTPP–8H]^+$	–	–	3.0	1.6
$[Fe/MnTPP–C_6H_6+2H]^+$	–	1	–	–
$[Fe/MnTPP–C_6H_6+H]^+$	–	1.5	–	–
$[Fe/MnTPP–C_6H_6]^+$	•	48.1	41.8	48.1
$[Fe/MnTPP–C_6H_6–H]^+$	–	3	–	–
$[Fe/MnTPP–C_6H_6–2H]^+$	•	27.8	38.6	35.4
$[Fe/MnTPP–C_6H_6–3H]^+$	–	1.9	–	–
$[Fe/MnTPP–C_6H_6–4H]^+$	•	14.4	18.8	15.7
$[Fe/MnTPP–C_6H_6–6H]^+$	•	1.6	0.8	0.8
$[Fe/MnTPP–2C_6H_5+H]^+$	–	0.8	–	–
$[Fe/MnTPP–2C_6H_5]^+$	•	42.7	35.7	40.1
$[Fe/MnTPP–2C_6H_5–H]^+$	•	3.1	–	–
$[Fe/MnTPP–2C_6H_5–2H]^+$	•	46.8	62.4	57.8
$[Fe/MnTPP–2C_6H_5–3H]^+$	–	2	–	–
$[Fe/MnTPP–2C_6H_5–4H]^+$	•	4.1	1.9	2.1

[a] % I is the normalized intensity of the ion relative to the other ions in the same channel according to formula % $I = R_1/\mathrm{sum}(R_x) \times 100$. Ions have been divided into three distinct channels according to the number of benzene residues lost (0, 1 or 2). The intensities are averaged over the range from 65 V to 130 V.

4.2.1. LDI/SID/FTMS

Early LDI/SID/FTMS studies of $[FeTPP]^+$ derived by laser desorption of [FeTPP]Cl showed losses of C_6H_6 and $2C_6H_5$ at low energies and additional molecular hydrogen losses at higher energies [19]. Although intensity versus energy curves were not recorded, the trends in the mass spectra produced at collision energies of 69 eV, 139 eV and 278 eV are similar to those recorded in our experiments by collision-induced dissociation (with nitrogen molecules) of the electrosprayed $[FeTPP]^+$ ions.

4.2.2. LDI/PD/FTMS

The ion dissociation products observed by the laser ablation/ionization of [FeTPP]Cl and [MnTPP]Cl [17] are included in Table 1. The dissociation features generally match those observed for $[FeTPP]^+$ and $[MnTPP]^+$ with ESI/CID. Three H_2 losses from the parent ion are indicated for photodissociation, whereas we have recorded up to four H_2 losses using ESI/CID. The further hydrogen losses leading ultimately to the formation of $[Fe/MnTPP–C_6H_6–6H]^+$ and $[Fe/MnTPP–2C_6H_5–4H]^+$ upon photodissociation also were observed using ESI/CID. The $[Fe/MnTPP–2C_6H_5–H]^+$ ion observed by photodissociation was minor and not seen with ESI/CID. Presumably, it arises by the loss of HCl, which is not possible in ESI/CID.

4.2.3. EI/MS

Table 1 shows many similarities between the results obtained with the EI/MS of [FeTPP]Cl and the ESI/CID of $[FeTPP]^+$; differences are apparent only for a few minor ions. Strong similarities are seen for the major dissociation products: the loss of even numbers of hydrogen atoms (presumably as H_2 molecules), loss of C_6H_5+H (presumably as benzene), and loss of $2C_6H_5$ (presumably as biphenyl). The CID of the electrosprayed ions causes more dissociation leading to loss of hydrogen molecules. Up to four H_2 molecules are lost sequentially by CID while up to two are lost by

EI, presumably due to the sequential input of energy by collision in the CID experiments.

The extent of hydrogen loss that is observed to accompany loss of C_6H_6 is similar in the two methods of excitation, as is the relative abundance. The relatively small losses of odd numbers of hydrogen that are seen only in the EI experiments may reflect the presence of Cl in the parent molecule that may be leaving as HCl upon electron impact. A similar situation, and presumably for the same reason, appears to apply to hydrogen loss that accompanies the loss of two phenyl groups (or $C_{12}H_{10}$). Again, relatively small accompanying losses of odd numbers of H atoms seen in the EI of [FeTPP]Cl are not seen in the CID of $[FeTPP]^+$.

4.3. Loss of hydrogen

The loss of an even number of hydrogen atoms is an overriding feature of the ESI/CID, as well as the EI, PD and SID experiments, and it is interesting to speculate about the origin of this loss. There are many H atoms in $[FeTPP]^+$ and $[MnTPP]^+$ that may be susceptible to dissociation. Although H atoms are available on the pyrrole rings for H_2 loss, H_2 loss is energetically unfavorable because of the strain that would be introduced in the formation of the resulting triple bonds in these rings.

The H atoms on the more peripheral phenyl rings also are available for H_2 loss. Indeed, free $C_6H_6^+$ ions are known to dissociate by loss of H or H_2. Formation of $C_6H_5^+ + H$ is more endothermic, $\Delta H^\circ f = 1348\ kJ\ mol^{-1}$, than formation of $C_6H_4^+$ (benzyne) + H_2, $\Delta H^\circ f = 1321\ kJ\ mol^{-1}$ [31]. So loss of H_2 would be favored and four consecutive H_2 losses from the $[Fe/MnTPP]^+$ parent ions might then lead to a product ion with four peripheral benzyne ligands.

4.4. Loss of benzene and biphenyl

The loss of benzene (C_6H_6) requires the pairing of a phenyl radical with one H atom. There are various H atoms on the pyrrole rings adjacent to the phenyl rings as well as on the other phenyl rings. The adjacent H atoms are likely to be preferred on steric grounds.

The loss of two phenyl radicals as biphenyl ($C_{12}H_{10}$) would require their recombination prior to dissociation. The phenyl groups that might recombine may be adjacent or opposite to each other. Recombination is favored thermodynamically.

Finally, it is not clear whether the metal M^{3+} cation (high spin unpaired electrons) might catalyze intramolecularly the recombination of H and C_6H_5 or two C_6H_5 radicals.

5. Conclusion

The bimolecular fragmentation of electrosprayed $[FeTPP]^+$ and $[MnTPP]^+$ ions induced by collisions with nitrogen molecules exhibits significant similarities with the unimolecular fragmentation induced by the electron impact or multiphoton dissociation of the parent FeTPPCl and MnTPPCl molecules. As one might expect, the modes of fragmentation are quite independent of the nature of the energy input. The presence of Cl appears to provide an extra dissociation channel when the parent molecule is ionized directly.

All the various ionization/mass spectrometry techniques that have been applied to the study of FeTPPCl and MnTPPCl provide mass spectral information useful in the elucidation of the structures of the parent porphyrin molecules. Primary ion dissociation products are dominated by the loss of C_6H_5, H (benzene) and $2C_6H_5$ (biphenyl). The sequential paired losses of 2H (hydrogen) up to four pairs or four molecules of hydrogen appear to arise from the four phenyl rings, while the H that is lost along with C_6H_5 may originate from the adjacent pyrrole ring.

Acknowledgments

Continued financial support from the Natural Sciences and Engineering Research Council (NSERC) of Canada is greatly appreciated. Financial support for this work was also provided by the National Research Council (NRC) of Canada and by MDS SCIEX. As holder of a Canada Research Chair in Physical Chemistry, DKB thanks the contributions of the Canada Research Chair Program to this research. The authors thank Dr. Voislav Blagojevic for useful discussions.

Appendix A. Supplementary data

Supplementary data associated with this article can be found, in the online version, at doi:10.1016/j.ijms.2008.10.018.

References

[1] K.M. Kadish, K.M. Smith, R. Guiliard (Eds.), The Porphyrin Handbook, vol. 1–10, Elsevier Science, Oxford, 2000.
[2] K.M. Kadish, K.M. Smith, R. Guiliard (Eds.), The Porphyrin Handbook, vol. 11–20, Elsevier Science, Oxford, 2003.
[3] G. Palmer, W.R. Dunham, J.A. Fee, R.H. Sands, T. Iizuka, T. Yonetani, Biochim. Biophys. Acta 245 (1971) 201.
[4] T.H. Moss, D. Petering, G. Palmer, J. Biol. Chem. 244 (1969) 2275.
[5] C. Moleski, T.H. Moss, W.H. Orme-Johnson, J.C.M. Tsibiris, Biochim. Biophys. Acta 214 (1970) 548.
[6] T.H. Moss, C. Moleski, J.L. York, Biochemistry 10 (1971) 840.
[7] T.H. Moss, D.C. Gould, A. Ehrenberg, J.S. Loehr, H.S. Mason, Biochemistry 12 (1973) 2444.
[8] J.W. Dawson, H.B. Gray, H.E. Hoenig, G.R. Rossman, J.M. Schredder, R. Wang, Biochemistry 11 (1972) 461.
[9] W.S. Caughey, Adv. Chem. Ser. 100 (1971) 248.
[10] B. Meunier, Chem. Rev. 92 (1992) 1411.
[11] K.S. Suslick, R.A. Watson, New J. Chem. 16 (1992) 633.
[12] J. Bernadou, G. Pratviel, F. Bennis, M. Girardet, B. Meunier, Biochemistry 28 (1989) 7268.
[13] M. Pitie, J. Bernadou, B. Meunier, J. Am. Chem. Soc. 117 (1995) 2935.
[14] P.R. Gardner, D.D.H. Nguyen, C.W. White, Arch. Biochem. Biophys. 325 (1996) 20.
[15] J.L. Hoard, G.H. Cohen, M.D. Glick, J. Am. Chem. Soc. 89 (1967) 1992.
[16] W.R. Scheidt, Acc. Chem. Res. 10 (9) (1977) 339.
[17] L.M. Nuwaysir, C.L. Wilkins, Anal. Chem. 61 (1989) 689.
[18] J.A. Castoro, L.M. Nuwaysir, C.F. Ijames, C.L. Wilkins, Anal. Chem. 64 (1992) 2238.
[19] C.F. Ijames, C.L. Wilkins, Anal. Chem. 62 (1990) 1295.
[20] S. Feil, M. Winkler, P. Sulzer, S. Ptasinska, S. Denifl, F. Zappa, B. Kräutler, T.D. Märk, P. Scheier, Int. J. Mass Spectrom. 255 (2006) 232.
[21] J.B. Fenn, J. Am. Soc. Mass Spectrom. 4 (1993) 524.
[22] V.E. Vandell, P.A. Limbach, J. Mass Spectrom. 33 (1998) 212.
[23] L.A. Hayes, A.M. Chappell, E.E. Jellen, V. Ryzhov, Int. J. Mass Spectrom. 227 (2003) 111.
[24] E.E. Jellen, A.M. Chappell, V. Ryzhov, Rapid Commun. Mass Spectrom. 16 (2002) 1799.
[25] G.J. Van Berkel, S.A. McLuckey, G.L. Glish, Anal. Chem. 63 (1991) 1098.
[26] G.J. Van Berkel, S.A. McLuckey, G.L. Glish, J. Am. Soc. Mass Spectrom. 3 (1992) 235.
[27] R.A. Yost, C.G. Enke, J. Am. Chem. Soc. 100 (1978) 2274.
[28] G.J. Francis, M. Forbes, D.A. Volmer, D.K. Bohme, Analyst 130 (2005) 508.
[29] J. Anichina, X. Zhao, D.K. Bohme, J. Phys. Chem. A 110 (2006) 10763.
[30] F. Paulat, V.K.K. Praneeth, C. Nather, N. Lehnert, Inorg. Chem. 45 (2006) 2835.
[31] H.M. Rosenstock, J. Dannacher, J.F. Liebman, Radiat. Phys. Chem. 20 (1982) 7.